Low-temperature measurements of the specific heat capacity of a thick ferroelectric copolymer film of vinylidene fluoride and trifluoroethylene

R. W. Newsome, Jr., S. Park, S.-W. Cheong, and E. Y. Andrei
Department of Physics and Astronomy, Rutgers University, Piscataway, New Jersey 08855, USA
(Received 26 September 2007; revised manuscript received 5 January 2008; published 4 March 2008)

The specific heat capacity c_p of a 110 μm thick and partially crystallized (~77%) ferroelectric copolymer film of vinylidene fluoride (PVDF) (~75 mol %) and trifluoroethylene (~25 mol %) was measured from 2 to 20 K. The temperature dependence of c_p/T^3 reveals a shallow hump, centered at ~5 K, consistent with non-Debye behavior of semicrystalline materials. These c_p data were used, in conjunction with previous measurements of the pyroelectric coefficient $|p'|$, to infer the temperature profile of the macroscopic Grüneisen parameter based on ratios of $|p'|/c_p$. Comparisons with similar data for PVDF are consistent with a correlation between anharmonicity of the interaction potential and excess specific heat capacity.

DOI: 10.1103/PhysRevB.77.094103 PACS number(s): 65.60.+a, 77.70.+a, 77.84.Lf, 77.84.Jd

I. INTRODUCTION

The copolymer vinylidene fluoride (PVDF)/trifluoroethylene (TrFE), with a composition of ~75 mol % PVDF and ~25 mol % TrFE, is ferroelectric[1] with well established pyroelectric[2–5] and piezoelectric[6] properties. Our measurements of the specific heat capacity c_p of a 110 μm thick sample of this copolymer extend from 2 to 20 K in intervals of 0.2 K and supplement the uneven coverage of prior measurements.[3,7,8] These data are used, in conjunction with prior measurements of the pyroelectric coefficient,[4,5] to infer the temperature dependence of the macroscopic Grüneisen parameter and to compare it with similar results deduced from available data for PVDF.[9] Our data also exhibit an excess value of c_p that exceeds the predictions of the Debye approximation and a hump in the plot of c_p/T^3. These are characteristic signatures of c_p for semicrystalline dielectrics at low temperatures.[10–12]

There is good scaling overlap between our low-temperature c_p data for PVDF/TrFE and those reported for PVDF by Privalko *et al.*[9] when they are normalized with their respective Debye values and plotted as a function of their Debye normalized temperatures. This implies that the temperature dependence of the excess specific heat capacity of the copolymer PVDF/TrFE is similar to that of its primary constituent.

Another noteworthy aspect of our c_p data is their overall agreement with independent estimates deduced from the sum of available c_p data for the two constituents of the copolymer,[13–16] weighted with their molar representation. This agreement supports the principle of additivity, formerly used to estimate c_p of linear fluoropolymers above ~40 K by adding contributions from their vibrational subunits.[17,18] It is also consistent with the behavior of some epoxies, whose c_p data are insensitive to chemical composition and cross-link densities.[19] However, it also implies that the specific heat of the copolymer in this temperature range is insensitive to its amorphous fraction. It was ~0.23 for our copolymer sample but ~0.50 and ~0, respectively, for c_p data from other sources for its two components, PVDF (Ref. 9) and TrFE.[14,15] This insensitivity to amorphous fraction was, however, not observed in c_p measurements of miscible blends of semicrystalline PVDF and amorphous poly(methyl methacrylate).[9]

The specific heat capacities of some polymers are in fact sensitive to the amorphous fraction, whereas others are not, and the reason for the difference is not well understood.[19–21] Quantitative resolution of the effects of amorphous content is confounded by ambiguities in defining the amorphous state and in measuring it. For example, the two-phase classification of polymer structures into purely crystalline and amorphous constituents is often a coarse oversimplification.[22–24] This inadequacy is reflected in significant differences for crystalline to amorphous ratios measured via different physical procedures, such as volume fraction, mass fraction, x-ray diffraction, small angle x-ray scattering, infrared absorption, and nuclear magnetic resonance.[22–24] There is also evidence for inhomogeneities in crystallinity[25] from measurements which show that orientational order decreases with increasing distance from the surface of stretched copolymer films whose composition and thickness are similar to those used for our c_p measurements.

Historically, the specific heat capacity was not expected to be sensitive to the amorphous fraction at low temperatures where the phonon wavelength is large compared to microscopic details of crystalline structure and amorphous voids.[10] Subsequent measurements, however, produced evidence to the contrary.[10,11,20,21] Many measurements also indicate that the amorphous environment is a primary source of non-Debye behavior of c_p for some polycrystalline materials at cryogenic temperatures. Characteristic manifestations are c_p values that deviate from a cubic temperature dependence and that exceed Debye predictions based on sound velocities in the media. This non-Debye behavior, known as excess specific heat capacity, is conjectured to be caused by low frequency vibrations of localized defects.[12,20,26,27] Recent attempts to understand this phenomenon have led to consideration of Bosonic modes in glassy phenomena,[28–31] whose long range van der Waals interactions are characteristically anharmonic.[27,32–36]

The Grüneisen parameter is a phenomenological measure of anharmonicity.[36] It was developed for crystalline solids but is often used, with varying levels of success, to characterize anharmonicity in other media, including polymers. On

a microscopic level, the Grüneisen parameter γ_n for each vibrational mode n of frequency ν_n is defined in terms of the change in ν_n due to a change in volume V:[19,37,38]

$$\gamma_n \equiv -\frac{d \ln \nu_n}{d \ln V}. \quad (1)$$

Thermodynamic relations may then be used to derive the macroscopic Grüneisen parameter γ, which relates the thermal expansion coefficient α to c_p for cubic and isotropic media:[19,38,39]

$$\alpha = \frac{1}{3}\frac{\rho}{\kappa_s} c_p \gamma, \quad (2)$$

where ρ represents the density and κ_s the adiabatic bulk modulus (inverse compressibility).

A derivation of Eq. (2) shows that γ is equal to a normalized sum of the microscopic Grüneisen parameters γ_n weighted with the specific heat capacity of each mode.[37–39] The microscopic parameters are usually assumed to be temperature independent, and the temperature dependence of the macroscopic parameter is then determined by the density of states, which determines the contribution of each mode to c_p.[37]

The temperature dependence of c_p is therefore a measure of the density of thermally induced excitations,[19] whereas γ reflects the asymmetry of the binding potentials as manifested by the anharmonic changes in their frequencies of oscillation.[19] Calculations of c_p are usually terminated with quadratic contributions from the interaction potential, which are inherently harmonic.[19,39,40]

At liquid helium temperatures, ρ and κ_s have a negligible temperature dependence. Under those conditions, the temperature dependence of γ depends only on α and c_p.[19,26,41] Fortunately, $\alpha(T)$ is readily accessible for our copolymer due to experimental confirmation that the temperature dependence of the pyroelectric coefficient of PVDF is dominated by α at cryogenic temperatures.[6,42,43] We assume that similar physical properties hold for our copolymer, PVDF/TrFE, whose primary component is PVDF. The parameters which define the pyroelectric coefficient are summarized in Appendix A.

Note that the parameters in Eq. (2) represent averages over vibrational modes for an isotropic medium. This is appropriate for the copolymer but not necessarily for PVDF, which must be mechanically stretched to produce the polarized β phase required for pyroelectric measurements. The stretching preferentially aligns the crystal domains along the stretch axis. Modified forms of Eq. (2) for uniaxially stretching are summarized in Appendix B. However, they were not used to interpret our measurements because the pyroelectric coefficients exhibited negligible differences in the temperature dependence for the unstretched copolymer compared to a uniaxially stretched sample of PVDF.

II. MEASUREMENT PROCEDURES

A. Sample

Most of our c_p measurements were conducted with a 110 μm thick film of PVDF/TrFE obtained from Measurement Specialties.[44] It had no metallic backings and was reported to consist of (~75 mol %) PVDF (~25 mol %) TrFE. The density and fractional crystalline content were approximately 1.78 g/cm^3 and ~0.77, respectively. The mass was limited to ~0.8 mg by the 9 mm^2 area of the calorimeter platform which supported it.

The high level of crystallinity (~77%) reported for a 230 μm sample was confirmed by a 2-Θ diffractometer measurement. The primary peak was sharp and narrow, at 20°, with a broad amorphous halo at smaller angles. This is consistent with results reported by Ikeda *et al.*[45] and Wong *et al.*[46] for a similar sample. Lorentzian functions provided adequate fits to our data. The ratio of areas in the two peaks yielded a crystallinity fraction of ~0.83, which is consistent with the estimate of ~0.77 from the supplier.[44] Two obvious sources of error in our x-ray measurements are scattering from the crystalline peak into the amorphous halo and an orientational bias in the scattering due to inadvertent stretching of the sample during processing.[23,25,47]

The copolymer PVDF/TrFE consists of polymerized chains of the monomer vinylidene fluoride (CH_2CF_2) interspersed with randomly distributed monomers of trifluoroethylene (CF_2CHF). The structure of TrFE differs from that of PVDF due to the replacement of a hydrogen atom by a larger fluorine atom. The resulting steric conflict causes a spontaneous transition to the β phase which has a net polarization per unit cell. Covalent bonding between carbon and fluorine atoms is the dominant source of electric dipole moments in both monomers.[1,4,6] Additional details about the structure of PVDF and PVDF/TrFE are provided by recent *ab initio* studies.[48–50] Note that PVDF requires mechanical stretching to create the polarized β phase required for pyroelectric measurements.[4]

B. Measurements

The specific heat capacity of the copolymer film was measured from 2 to 20 K with a general purpose calorimeter from Quantum Design.[51,52] It utilizes the Hwang algorithm[53] to extract heat capacity data from the thermal response of the sample to heat pulses. A minute amount of Apiezon-N grease[54] provided the thermal interface between the sample and the substrate of the support platform. The specific heat capacity of the addenda (measured with the grease in place before the sample was positioned on it) was always less than that of the sample but comparable in magnitude. Therefore, addenda runs were as extensive as those with the sample in place in order to minimize statistical errors.

Measurements were repeated multiple times at each temperature, which was monotonically increased (i.e., heating) or decreased (i.e., cooling) over the full temperature range. The 110 μm thick sample and its addenda were measured over both heating and cooling sequences. They revealed a small hysteresis in the form of a broad hump in the heating data which was similar in shape and temperature range for the addenda and the sample plus addenda runs. The hysteresis from ~2.5 to ~5 K never exceeded 10% of the average value of c_p. This was attributed to helium gas contamination due to a malfunction of the calorimeter.[51] A similar problem

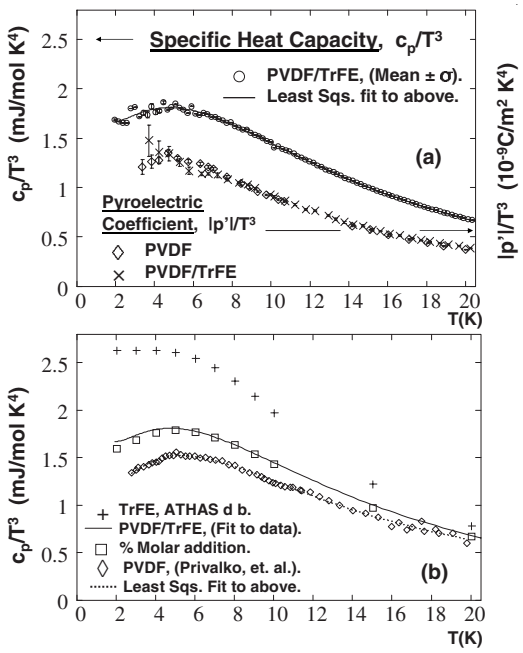

FIG. 1. (a) Data for c_p/T^3, averaged over the heating and cooling runs with the 110 μm thick sample of PVDF/TrFE. It also contains plots of $|p'|/T^3$ from previous measurements of the pyroelectric coefficient for PVDF/TrFE (Ref. 5) and PVDF (Ref. 4). The solid curve represents a least squares fit to the specific heat capacity data. (b) The same fit to c_p/T^3 for the copolymer, compared with results (square symbols) deduced from the sum of c_p for its two constituents. The data for PVDF are from Privalko *et al.*[9] and those for TrFE are from the ATHAS database (Refs. 13–15).

was reported by another user of a Quantum Design calorimeter.[55] Although the hysteresis was eliminated with additional activated charcoal in the sample chamber, we were unable to improve on the data reported here. Our addenda subtraction provided a first order correction to the helium problem, and we therefore chose to average our heating and cooling data. There were inherent difficulties in obtaining a good thermal contact between the substrate and the polymer films, because random stresses during production and subsequent cutting of the films apparently caused elastic distortions during the cooling process.[56,57]

Measurements were initially performed with a 230 μm thick sample, but they were conducted before the helium gas contamination problem was discovered and contain only a heating sequence. They are in general agreement with c_p measurements from the 110 μm thick sample but tend to be about one mean standard deviation larger, and were therefore not included in the processed results below 20 K.

III. PRESENTATION OF THE DATA

A. Temperature dependence of c_p/T^3

Data for the 110 μm thick sample, averaged and normalized with T^3, are plotted with circles in Fig. 1(a). The vertical error bars show the range of one standard deviation above and below the mean values for c_p/T^3, and most are too small to be resolved in this plot. The solid curve is a least squares fit to these data. All the c_p data are expressed in units of monomer moles, which are, respectively, 64.03 and 68.53 g/mol for PVDF and PVDF/TrFE with molar concentrations of (0.75/0.25).

Figure 1(a) also contains plots of previously measured pyroelectric coefficients, normalized by T^3, for the copolymer PVDF/TrFE (Ref. 5) and PVDF.[4] They have an almost identical dependence on temperature, which resembles that of the normalized specific heat capacity. The pyroelectric data from PVDF also exhibit a distinct peak at ~4 K, whereas the noisier data from the copolymer hint at the possibility of a peak at lower temperatures.

The rectangular symbols in Fig. 1(b) show the agreement between our results for c_p/T^3 of the copolymer and values based on molar weighted sums of c_p for the two primary constituents of the copolymer. The sources of the latter were recent measurements by Privalko *et al.*, of c_p for PVDF (Ref. 9) (plotted with diamond symbols) and estimates of c_p for TrFE from tabulations in the ATHAS database[14] (plotted with crosses). The copolymer consisted of ~75 mol % PVDF. Tabulations of c_p for TrFE in the ATHAS database[14] were extrapolated from data at higher temperatures using the Tarasov approximation for Debye crystalline media.[58] Note that c_p/T^3 values for the TrFE data are flat below ~4 K because the Tarasov approximation reduces to a cubic (Debye) temperature dependence there. The data for PVDF also show a peak at ~5.4 K.

The more distinctive hump in the PVDF data compared to those for the copolymer, is consistent with established trends that correlate enhanced non-Debye behavior with increased values of amorphous content. Note that the amorphous fraction of the PVDF and PVDF/TrFE were, respectively, ~0.5 and ~0.23.

1. Comparison with Debye prediction for c_p

The low-temperature Debye prediction of c_D/T^3 for crystalline matter is[59]

$$\frac{c_D}{T^3} = \frac{2}{15}\frac{\pi^2}{\hbar^3}\frac{k_B^4}{\rho}\left(\frac{1}{v_l^3} + \frac{2}{v_t^3}\right), \tag{3}$$

where v_l and v_t represent, respectively, the longitudinal and transverse sound velocities and k_B is the Boltzmann constant.

The sound velocities of lamellar crystalline films of PVDF/TrFE at 10 K, averaged over longitudinal and transverse components, are, respectively, 2672 and 1495 m/s.[60,61] These velocities were extrapolated to 0 K using rates of $dv_l/dT = -2.5$ ms^{-1} K^{-1} and $dv_t/dT = -2.0$ ms^{-1} K^{-1}.[9] The resulting average (Debye) sound velocity v_D at 0 K for PVDF/TrFE is 1642 m/s, compared with 1716 m/s reported for PVDF.[9] The velocity v_D is defined as[59]

$$\frac{1}{v_D^3} = \frac{1}{3}\left(\frac{1}{v_l^3} + \frac{2}{v_t^3}\right). \tag{4}$$

Note that the generic product ρv^3 is invariant to corrections for thermal length contraction.[62]

The velocity v_D of the copolymer is about 4% smaller than that of PVDF (Ref. 9) in spite of respective crystallinity

factors of ~0.77 and ~0.5. The sound velocity in the copolymer is slower, presumably because its crystals are localized in lamellar domains that are acoustically isolated from each other.[61]

The cutoff frequency of acoustic phonons defines the Debye temperature Θ_D, which depends on the choice of the vibrating unit, customarily chosen as the repeating unit for polymer chains.[59] The parameters c_D and Θ_D are related by

$$\frac{c_D}{T^3} = \frac{4}{5}\frac{\pi^4}{\Theta_D^3} N_o n k_B, \tag{5}$$

where N_o is the Avogadro number and n is the number of degrees of freedom per vibrating unit. For fluoropolymers with six atoms per repeating unit, there are four acoustic normal modes at low temperatures.[59]

In the Tarasov approximation for elongated polymers,[19,58,59]

$$\Theta_D^3 = \theta_1 \theta_3^2, \tag{6}$$

where θ_3 and θ_1 are, respectively, the cutoff frequencies for three-dimensional (3D) and one-dimensional (1D) propagation.

For $T \ll \theta_3$:[59]

$$\frac{c_D}{T^3} = \frac{4}{5}\frac{\pi^4}{\theta_1 \theta_3^2} N_o n k_B, \tag{7}$$

Evaluation of Eq. (3) for the copolymer,[61] using $\rho = 1.88\ g/cm^3$, yields $c_D/T^3 = 1.01\ mJ/mol\ K^4$ and $\Theta_D = 137$ K. The corresponding values, based on sound velocities for PVDF,[9] are, respectively, $0.877\ mJ/mol\ K^4$ and 143.5 K. Some of the difference in the excess specific heat capacity observed for PVDF and PVDF/TrFE is undoubtedly due to differences in chemical composition which alters binding potentials of vibrating subunits.[16] Some compensation for such effects might be attained by scaling the specific heat capacity and temperature by their Debye values, as proposed by Sokolov *et al.*[63] This scaling procedure was applied to plots of c_p versus T in Fig. 2 for our PVDF/TrFE data and those for PVDF reported by Privalko *et al.*[9] The overlap is surprisingly good even though the Debye normalizations, deduced from sound velocity data, do not include the Tarasov correction,[58] which approximates the presumed transition from 1D to 3D phonon propagation in polymer chains as they are cooled from intermediate temperatures to absolute zero.

Equation (7) contains the Tarasov corrected form of the Debye approximation at low temperatures. Reported values of θ_3 and θ_1 for PVDF are 95 and 357 K, respectively.[59] Similar estimates from our measurements of PVDF/TrFE are, respectively, 68 and 460 K. Attempts to use these scaling parameters yielded poor overlap, as did use of the unscaled temperature without the Θ_D normalizations. The tentative conclusion is that the temperature range for our data straddles the two Tarasov regimes and that our original attempt yields a functional compromise.

Figure 2 also contains scaling of c_p data for polytetrafluoroethylene (PTFE) (known as Teflon),[62,64,65] for which the two hydrogen atoms in each repeat unit of PVDF are replaced with fluorine to form a repeat unit, CF_2CF_2. Good overlap with the scaled data for PVDF and PVDF/TrFE is readily attained only when Θ_D is calculated via Eq. (5), with two rather than the four acoustic modes customarily assigned to fluoropolymers at low temperature.[16,59] The shape and vertical position of the scaled data for PTFE are only moderately sensitive to changes within the ~10% uncertainty in c_D calculated from available velocity of sound data, but the horizontal position is visibly sensitive to differences in Θ_D deduced for different numbers of acoustic modes. This latter sensitivity is readily apparent in the scaled data for PTFE, whose normalization factor c_D was shifted to the lower range of its estimated uncertainty in order to facilitate comparison of its shape with the other data plotted in Fig. 2.

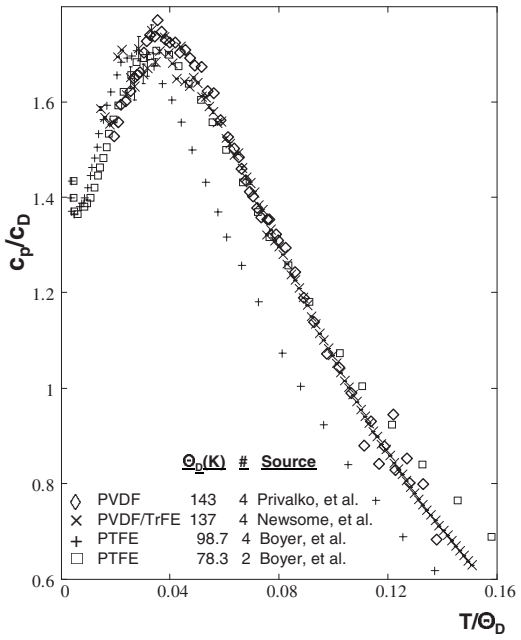

FIG. 2. Comparisons of the specific heat capacity of PVDF (Ref. 9), PVDF/TrFE, and PTFE (Teflon) (Ref. 64), scaled with their respective Debye values, deduced from velocity of sound data (Refs. 9 and 60–62). The data are plotted as a function of their Debye normalized temperature Θ deduced from Eq. (5) for specific numbers of acoustic modes, denoted by the column label # in the legend.

Previous c_p measurements of fluoropolymers[16] indicate that the three-dimensional interchain interaction decreases when hydrogen atoms are replaced by fluorine, with the exception of TrFE (CF_2CHF) and PTFE (CF_2CF_2). We have no explanation why two acoustic modes yield a Θ_D that provides a superior scaling fit to c_p data for PTFE. This behavior may indicate, however, that the temperature dependence of non-Debye contributions to c_p for fluoropolymers possesses a common scaling parameter.

IV. TEMPERATURE DEPENDENCE OF THE PYROELECTRIC COEFFICIENTS

Figure 3 displays previous measurements of the pyroelectric coefficients $|p'|$ for 10 μm thick samples of PVDF and

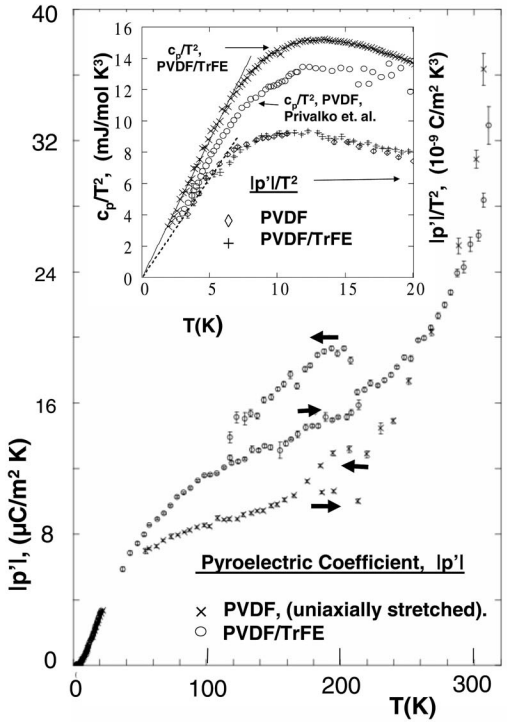

FIG. 3. Comparisons of the pyroelectric coefficients measured for uniaxially stretched PVDF (Ref. 4) and the unstretched copolymer PVDF/TrFE (Ref. 5). The arrows adjacent to the hysteresis loops show the directions of the quiescent temperature changes near the well known glass transition regions in the vicinity of 200 K. The inset contains data from Fig. 1, normalized with T^2 rather than T^3. The circular symbols represent c_p/T^2 for PVDF from Privalko *et al.* (Ref. 9), whereas the crosses represent similar averages of our data for a 110 μm thick sample. The solid line is a linear least squares fit to the latter data from 2 to 8 K. Also included in the inset are averages of $|p'|/T^2$ for PVDF and the copolymer PVDF/TrFE. The dashed line is a linear least squares fit to these data from 3 to 6 K.

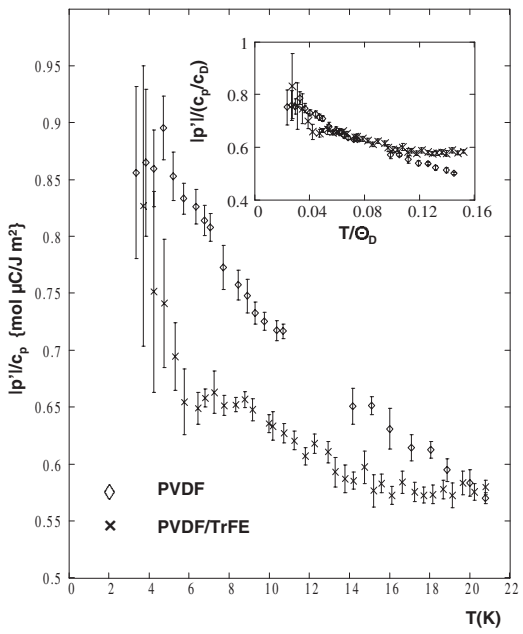

FIG. 4. Inferred temperature dependence of the Grüneisen parameters, deduced from the ratios of the pyroelectric coefficient to the specific heat capacity, as described in the text. The insert displays the same ratios with c_p scaled by c_D and plotted as a function of the Debye scaled temperature.

PVDF/TrFE, with the same properties as those used to acquire the c_p/T^3 data in Fig. 1.[4,5] The similarity in the temperature dependence of $|p'|$ from ~3 to ~20 K indicates that the alignment of the stretched PVDF sample does not significantly affect the values of $|p'|/c_p$ over the low-temperature range of interest here. That similarity does not exist at higher temperatures, however, especially in the vicinity of the primary glass transition near ~200 K.

The inset in Fig. 3 shows the data from Fig. 1 normalized with T^2 rather than T^3. Note that the temperature dependence of $|p'|/T^2$ exhibits a break in the vicinity of ~6 K,[4,5] which does not appear in our measurements of c_p/T^2 for PVDF/TrFE or for those of PVDF.[9] That difference undoubtedly reflects the dependence of $|p'(T)|$ on $\alpha(T)$, which is inherently more sensitive to anharmonicity than c_p, whose interaction potential is dominated by quadratic terms. On the other hand, the T^2 normalization overemphasizes the dominant cubic temperature dependence of our data because linear fits over the lower range of temperatures have intercepts that are statistically consistent with zero.

V. INFERRED TEMPERATURE DEPENDENCE OF THE MACROSCOPIC GRüNEISEN PARAMETER

The data in Fig. 4 show our estimates of the temperature dependence of γ for PVDF/TrFE and PVDF, inferred from the ratios of $|p'|/c_p$. Those ratios consist of the pyroelectric data from Fig. 1 divided by the least squares fit to the corresponding data for c_p. The steep rise in the noisy data for the copolymer may indicate a corresponding peak below 4 K. The ratio will inevitably decrease again at lower temperatures due to tunneling between localized anomalies in amorphous media, which contributes to c_p but not α.[19] For higher temperatures, the plotted ratios for the copolymer fall off significantly faster than those for PVDF, which is consistent with the lower amorphous fraction for the copolymer sample.

Peaks in the $\gamma(T)$ have also been reported for other amorphous polymers in the vicinity of ~10 K.[19,41] This is plausible because γ is typically small below the tunneling regime, in the vicinity of ~1 K, and increases as interchain interaction becomes dominant at higher temperatures. Those interactions are propagated by van der Waals forces, whose potentials exhibit anharmonic asymmetries that increase with increasing excitation, causing a steep rise in γ for amorphous media. Intrachain interactions, mediated by covalent bonds with more symmetric potentials, become dominant above ~10 K. The consequent reduction in γ may also be markedly increased by bending vibrations which can reduce the thermal expansion coefficient, even to the point of changing its sign.[19]

Figure 4 shows a steep drop in the temperature dependence of γ for the highly crystalline copolymer PVDF/TrFE. It is similar to early results attained for crystalline chains of

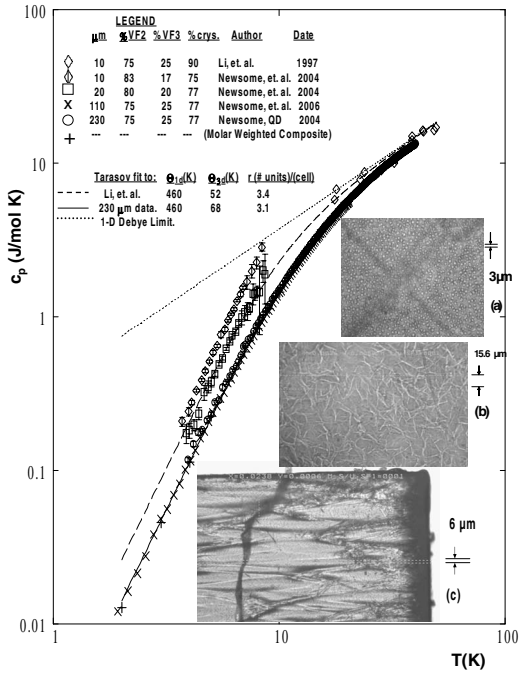

FIG. 5. Logarithmic plots of c_p for PVDF/TrFE and some optical microscope pictures of some of the thin films. The thicknesses of samples (a), (b), and (c) were, respectively, 20, 110, and 230 μm. The measurements by Li and Chigashi were taken with an ac calorimeter (Ref. 3). The column labels %VF2 and %VF3, represent, respectively, the molar percentage of PVDF and TrFE in the sample.

tellurium, which were used to model polymer behavior.[37,66] Subsequent measurements, however, showed a slight rise in γ for tellurium from $\sim$2 to $\sim$6 K.[67]

Primary measurements of γ for isotropic polyethylene (CH_2CH_2), deduced from direct measurements of its thermal expansion coefficient, exhibit a flat temperature dependence from $\sim$2.5 to $\sim$10 K, with a steep falloff at higher temperatures.[26] Reproducible measurements of γ for semicrystalline polymers are especially difficult due to the dependence of physical properties on their thermal processing history.[68]

The inset in Fig. 4 displays ratios of $|p'|/c_p$ using Debye normalizations for c_p and T. They infer the same temperature dependence for γ from $\sim$7 to $\sim$14 K, with significant deviations at lower and higher temperatures. The flat temperature dependence above $\sim$14 K of these ratios for the copolymer compared to PVDF is consistent with less anharmonicity for more crystalline materials until that trend is reversed below $\sim$6 K.

VI. MORPHOLOGICAL EFFECTS

Several sets of the data displayed in Fig. 5 were fitted to simplified Tarasov algorithms. They consist of a 1D and a 3D Debye function, with bending modes neglected. The fits reveal their sensitivity to the associated Debye temperatures. They are not exhaustive because the Debye temperatures Θ_{1D} and Θ_{3D} are not independent in the low-temperature limit of the Tarasov model.[65] In addition, the 1D Debye function has a dominant linear dependence at higher temperatures, which decreases the sensitivity of the predicted value of c_p to Θ_{1D}. Therefore, Θ_{1D} was set to a plausible value of 460 K, based on prior measurements,[3] while Θ_{3D} and the normalization coefficient r, which represents the effective number of oscillators per unit cell,[3] were varied to optimize a visual fit to the data, as tabulated in Fig. 5.

Our fits were insensitive to variations of less than about 5 K in Θ_{3D}, when the other two variables were held fixed. Therefore, a more precise fit is not warranted. It is of interest to note the similarity of our values for Θ_{3D} with previously published values of 53 and 69 K, respectively, obtained from photoemission and neutron diffraction measurements of this copolymer for sample thicknesses of 5 and 50 molecular layers, respectively.[69]

Additional data from prior measurements of c_p for thinner films are also included in Fig. 5. The data from the thinner samples were previously measured from 4 to 8 K with a homemade calorimeter,[7,8] which utilized the Hwang algorithm for data extraction.[53] The temperature range of that device was limited to the vicinity of 6 K. Although the sampling rate was several orders of magnitude slower than that for the Quantum Design instrument, it did permit c_p to be measured for a 0.6 mg sample of a 10 μm thick film. The specific heat capacity of films of that thickness was not measurable with the Quantum Design calorimeter because the sample mass was below the sensitivity limit of $\sim$1 mg.[51] For example, an attempted measurement of c_p with a 30 μm thick sample did not yield stable results.

Insets (a), (b), and (c) in Fig. 5 display the surface morphologies of the 20, 110, and 230 μm thick copolymer films. Many of the same vesicular-type structures in the thinner, 10 and 20 μm thick, films are clearly visible from both of their surfaces. The other side of the 230 μm thick film, however, is almost opaque and exhibits a negligible amount of structure. Optical examination of this film with resolution of $\sim$0.1 μm showed only a fuzzy grainy structure with no evidence of the $\sim$3 μm circular structures seen in the thinner films. All pictures were taken in white light with a Leica (Leitz LABORLUX S) microscope.

Circular structures, several microns in diameter, were previously observed in 8 μm thick films of PVDF, using a scanning electron microscope.[70] Similar studies of the copolymer PVDF/TrFE, composed of 70 mol % PVDF, show networks of tangled bundles whose thicknesses and pores increase with increasing crystallization temperature.[2,70,71] The formation and growth of lamellas and spherulite structures are complex phenomena which reflect the thermal history during the production process.[72–75] Further investigation of their effect on measurements of c_p obviously requires precise specification of the crystalline state of the system.

Several other factors can also contribute to the trend (displayed in Fig. 5) toward values of c_p that are larger for thinner samples.[7] Plausible contributors could be surface contaminants and damage to the perimeters of the samples when they are cut. The ragged edge on the right side of inset (c) in Fig. 5 demonstrates an extreme case of the damage caused by cutting the sample with dull shears. Razor cuts are preferable, but even they tend to fray strands of the copolymer,

whose pointed ends accentuate the strength of electric fields produced by pyroelectric surface charge induced by temperature changes.[76] The thermally induced charge and associated electric fields are largest in the vicinity of room temperature, where $|p'|$ is several orders of magnitude larger than at the temperature of liquid helium.[5,4] These fields may elongate and proliferate the frayed strands in a process known as spinning.[77,78] Although surface charging of a pyroelectric can be avoided by the use of metallized coatings, those coatings are also sources of contamination and damage, and they make precise addenda corrections more difficult.[3]

Another potential problem in our measurements involves the grease that provided thermal interface between the copolymer films and the substrate. Silicon vacuum grease was used to attach the 10 and 20 μm thick films to the substrate of our homemade calorimeter. Although visual examination before and after data collection showed no signs of interaction with the films, that grease is not rated for use at cryogenic temperatures.[79] The thicker samples were attached to the substrate of the Quantum Design calorimeter with Apiezon-N grease, which is rated for use at cryogenic temperatures. A potentially insidious problem from use of any grease is the possibility of absorption of the grease at room temperature, which might then act as a filler at cryogenic temperatures. Therefore, the cryostats were promptly cooled after the films were placed on the grease.

VII. SUMMARY

Low-temperature measurements of the specific heat capacity of PVDF/TrFE were extended, with improved accuracy, from 20 to 2 K. They are consistent with molar weighted sums of c_p extrapolated from measurements at higher temperatures for the two primary constituents of the copolymer.

The temperature dependence of c_p/T^3 for the copolymer PVDF/TrFE exhibits a small but distinct deviation from the cubic temperature dependence predicted by the Debye approximation, from ~2 to ~8 K. Although the excess for the copolymer is smaller than that observed for PVDF over the same temperature range,[9] it exhibits the same temperature dependence when the data are scaled by their respective Debye parameters for c_D and Θ_D. If the source of the excess is the amorphous content,[10,19,26] then our results indicate that the normalized strength and temperature dependence of the excess c_p are the same for the two polymers considered here. This indicates that samples of the copolymer with 100% crystallinity, which have been produced,[60,61] would exhibit no excess specific heat capacity.

Independent evidence that the temperature dependence of $p'(T)$ reflects that of the thermal expansion coefficient $\alpha(T)$ for PVDF and PVDF/TrFE at liquid helium temperatures implies that the temperature dependence of the ratio $|p'|/c_p$ reflects that of the macroscopic Grüneisen parameter $\gamma(T)$ for those polymers in that temperature regime. The PVDF data for that ratio exhibit a sustained, approximately linear decrease from ~5 to 20 K. This contrasts with a sharp decrease at ~5 K, followed by comparatively flat behavior out to 20 K for PVDF/TrFE. These reflect differences in $c_p(T)$ as well as $|p'|(T)$. The latter is almost identical for the two materials, except for an anomalous dip in $|p'|$ near ~6 K and slightly higher values above ~16 K for the copolymer. Although the microscopic γ_n for each mode is defined in terms of a fractional frequency shift, which is patently anharmonic, that definition has no temperature dependence. In that phenomenological model, the inferred temperature dependence of the macroscopic Grüneisen parameter γ is due to temperature dependent activation of the various modes. The specific heat capacity, on the other hand, is dominated by the harmonic quadratic term in the expansion of the interaction potential.[39] It can, nevertheless, affect the temperature dependence of γ via the density of states that orchestrates the activation of the individual modes. Therefore, the next step in interpreting our data would be to measure this density of states and identify the participating modes. Tests should also be devised to validate models that attempt to relate the excess specific heat capacity to the glassy behavior of amorphous media at low temperatures.[31]

The data from the thinner samples, 10 and 20 μm thicknesses, allude to the possibility that surface effects and morphologies may affect their specific heat capacities. Exploration of such effects remains a challenge for the future.

ACKNOWLEDGMENTS

The authors gratefully acknowledge the generous help of D. Halvorsen and M. L. Thompson of Measurement Specialties[44] for providing the copolymer samples. Helpful consultation with R. Black of Quantum Design is also gratefully acknowledged.[51] Thanks are also due to J. Scheinbeim for discussions about the crystalline structure of the copolymer and to W. E. Mayo for his diffraction x ray of a sample. This work was supported by Grants No. NSF-DMR-0102692, No. NSF-DMR-0520471, and No. DOE-DE-FG02-99ER45742.

APPENDIX A

A general expression for the pyroelectric coefficient is obtained by expanding the thermodynamic equation of state (i.e., the Gibbs free energy:[80,82,83])

$$|p'| \equiv \frac{1}{A}\left(\frac{\partial Q}{\partial T}\right)_{\boldsymbol{\Sigma},\tilde{\mathbf{E}}=0} = \left(\frac{\partial P_3}{\partial T}\right)_{\eta,\tilde{\mathbf{E}}=0} + d_{3jk}C_{jklm}\alpha_{lm} + P_3\alpha_A. \tag{A1}$$

The left side of this equation defines the magnitude of p' under conditions of no external mechanical stress $\boldsymbol{\Sigma}$ or electric fields $\mathbf{E}$. The first term on the right is the primary pyroelectric coefficient p_{I}. It represents the thermal response of the normal polarization component P_3 under conditions of no strain η (i.e., fixed macroscopic dimensions). There is convincing evidence that the primary coefficient is negligible for PVDF and PVDF/TrFE.[6,42,43]

The second term on the right represents the secondary or piezoelectric contributions p_{II}. It is due to thermally induced changes in macroscopic dimensions and consists of a product of the direct piezoelectric coefficient $\mathbf{d}$ (which relates the

change in polarization induced by stress), the elastic stiffness tensor **C** (which relates stress to strain), and the thermal expansion coefficient α. The low-temperature dependence of p_{II} is dominated by the thermal expansion coefficient α because the multiplicative compliance coefficients are typically constant at very low temperatures.[6,80,81]

The third term contains the two-dimensional thermal expansion coefficient, $\alpha_A = \alpha_1 + \alpha_2$, where α_1 and α_2 are the coefficients along principal axes of the surface. It corrects for the fact that typical measurements are of the surface charge and not the surface charge density.[82–84] It is estimated to be negligible at cryogenic temperatures.[4]

APPENDIX B

For uniaxial stretching, with symmetry assumed in the plane perpendicular to the stretched axis, the Grüneisen relations become[19,26,37]

$$\gamma_\perp = [(C_{11} + C_{12})\alpha_\perp + C_{13}\alpha_\parallel]/\rho c_p \tag{B1}$$

and

$$\gamma_\parallel = [2C_{13}\alpha_\perp + C_{33}\alpha_\parallel]/\rho c_p. \tag{B2}$$

The indices for the adiabatic stiffness matrix elements C_{ij} are labeled (3) for the stretched or parallel axis and (1) and (2) for the axes perpendicular to it. The PVDF sample was uniaxially stretched during production, and isotropy is assumed for planes perpendicular to the stretched direction.

The inverse of the previous equations yields expressions for $\alpha_\parallel$ and $\alpha_\perp$ in terms of corresponding Grüneisen parameters, weighted with inverse adiabatic compliance matrix elements S_{ij}:[19,26,37]

$$\alpha_\perp = [(S_{11} + S_{12})\gamma_\perp + S_{13}\gamma_\parallel]\rho c_p \tag{B3}$$

and

$$\alpha_\parallel = [2S_{13}\gamma_\perp + S_{33}\gamma_\parallel]\rho c_p. \tag{B4}$$

The resulting temperature dependence inferred from the pyroelectric coefficient for PVDF is therefore a weighted composite of $\gamma_\parallel$ and $\gamma_\perp$.

Comparisons of the temperature dependence of $\gamma(T)$ for PVDF/TrFE and PVDF are nevertheless simplified for several reasons. One is that 50% of the PVDF sample was amorphous, with an isotropy that is presumably not affected by the stretching process. In addition, the value of $\alpha(T)$ related to the crystalline part of the sample is probably dominated by the perpendicular component, as indicated by low-temperature measurements of polyethylene.[26] The most compelling simplification is that the low-temperature dependence exhibited by the pyroelectric coefficient $|p'|$ of PVDF is almost identical, with several small exceptions, to that of the copolymer PVDF/TrFE.[4,5]

[1] K. Tashiro, in *Ferroelectric Polymer: Chemistry, Physics, and Applications*, edited by H. S. Nalwa (Marcel Dekker, New York, 1995), p. 63.
[2] K. Kimura and H. Ohigashi, Jpn. J. Appl. Phys., Part 1 **25**, 383 (1986).
[3] G.-R. Li and H. Ohigashi, Jpn. J. Appl. Phys., Part 1 **31**, 2495 (1992).
[4] R. W. Newsome, Jr. and E. Y. Andrei, Phys. Rev. B **55**, 7264 (1997).
[5] R. W. Newsome, Jr. and E. Y. Andrei, Bull. Am. Phys. Soc. **44**, 1839 (1999).
[6] R. G. Kepler, in *Ferroelectric Polymers: Chemistry, Physics, and Applications*, edited by H. S. Nalwa (Marcel Dekker, New York, 1995), p. 183.
[7] R. W. Newsome, Jr. and E. Y. Andrei, Phys. Rev. B **69**, 064105 (2004).
[8] R. W. Newsome, Jr. and E. Y. Andrei, Rev. Sci. Instrum. **75**, 104 (2004).
[9] V. P. Privalko, B. Ya. Gorodilov, N. A. Rekhteta, E. G. Privalko, A. Bartolotta, G. Carini, G. D. D'Angelo, and G. Tripodo, Philos. Mag. B **82**, 467 (2002).
[10] R. O. Pohl, in *Amorphous Solids: Low Temperature Properties*, edited by W. A. Phillips (Springer-Verlag, Berlin, 1981).
[11] R. C. Zeller and R. O. Pohl, Phys. Rev. B **4**, 2029 (1971).
[12] R. O. Pohl, X. Liu, and EunJoo Thompson, Rev. Mod. Phys. **74**, 991 (2002).
[13] B. Wunderlich, J. Therm. Anal. **46**, 643 (1996).
[14] ATHAS, the advanced thermal analysis system (http://athas.piz.edu.pl).
[15] U. Gaur, B. B. Wunderlich, and B. Wunderlich, J. Phys. Chem. Ref. Data **12**, 29 (1983).
[16] W. K. Lee and C. L. Choy, J. Polym. Sci., Polym. Phys. Ed. **13**, 619 (1975).
[17] B. Wunderlich and L. D. Jones, J. Macromol. Sci., Phys. **3**, 67 (1969).
[18] K. C. Wong, F. C. Chen, and C. L. Choy, Polymer **16**, 649 (1975).
[19] G. Hartwig, *Polymer Properties at Room and Cryogenic Temperatures* (Plenum, New York, 1994).
[20] C. L. Choy, M. Hug, and D. E. Moody, Phys. Lett. **54A**, 375 (1975).
[21] J. E. Tucker and W. Reese, J. Chem. Phys. **46**, 1388 (1967).
[22] G. Strobl, *The Physics of Polymers* (Springer-Verlag, Berlin, 1997).
[23] L. E. Alexander, *X-Ray Diffraction Methods in Polymer Science* (Wiley-Interscience, New York, 1969).
[24] R.-J. Roe, *Methods of X-Ray and Neutron Scattering in Polymer Science* (Oxford University Press, Oxford, 2000).
[25] M. A. Barique, M. Sato, and H. Ohigashi, Polym. J. (Tokyo, Jpn.) **33**, 69 (2001).
[26] C. K. White and C. L. Choy, J. Polym. Sci., Polym. Phys. Ed. **22**, 835 (1984).
[27] G. Carini, G. D'Angelo, G. Tripodo, A. Bartolotta, and G. DiMarco, Phys. Rev. B **54**, 15056 (1996).
[28] B. Terziyska, A. Czopnik, E. Vateva, D. Arsova, and R. Czopnik, Philos. Mag. Lett. **85**, 145 (2005).
[29] M. A. Ramos, Philos. Mag. **84**, 1313 (2004).

[30] V. Lubchenko and P. G. Wolynes, Phys. Rev. Lett. **87**, 195901 (2001).
[31] N. G. C. Astrath, A. C. Bento, M. L. Baesso, E. K. Lenzi, and L. R. Evangelista, Philos. Mag. **87**, 291 (2007).
[32] C. Talón, M. A. Ramos, S. Vieira, G. J. Cuello, F. J. Bermejo, A. Criado, M. L. Senent, S. M. Bennington, H. E. Fischer, and H. Schober, Phys. Rev. B **58**(2), 745 (1998).
[33] C. A. Angel, Science **267**, 1924 (1995).
[34] A. Bartolotta, G. Carini, G. D'Angelo, G. D. Marco, Ya. Gorodilov, E. G. Privalko, V. P. Privalko, B. N. A. Rekhteta, and G. Tripodo, J. Phys.: Condens. Matter **15**, S987 (2003).
[35] G. Carini, G. Carini, G. D'Angelo, G. Tripodo, A. Bartolotta, and G. D. Marco, J. Phys.: Condens. Matter **18**, 10915 (2006).
[36] G. Carini, G. Carini, G. D'Angelo, G. Tripodo, A. Bartolotta, and G. Salvato, Phys. Rev. B **72**, 014201 (2005).
[37] T. H. K. Barron, J. G. Collins, and G. K. White, Adv. Phys. **29**, 609 (1980).
[38] N. W. Ashcroft and N. D. Mermin, *Solid State Physics* (Harcourt, Brace, New York, 1976).
[39] J. M. Ziman, *Principles of the Theory of Solids* (Cambridge University Press, Cambridge, 1972).
[40] H. Ibach and H. Lüth, *Solid State Physics* (Springer-Verlag, Berlin, 1991).
[41] C. A. Swenson, Rev. Sci. Instrum. **68**, 1312 (1997).
[42] R. G. Kepler and R. A. Anderson, J. Appl. Phys. **49**, 4918 (1978).
[43] R. G. Kepler and R. A. Anderson, Mol. Cryst. Liq. Cryst. **106**, 345 (1989).
[44] Measurement Specialties; 950 Forge Avenue, Norristown, PA 19403.
[45] S. Ikeda, Z. Shimojima, and M. Kutani, Ferroelectrics **109**, 297 (1990).
[46] Y. W. Wong, N. M. Hui, E. L. Ong, H. L. W. Chan, and C. L. Choy, J. Appl. Polym. Sci. **89**, 3160 (2003).
[47] C. R. Desper and R. S. Stern, J. Polym. Sci., Part B: Polym. Lett. **5**, 893 (1967).
[48] H. Su, A. Strachan, and W. A. Goddard III, Phys. Rev. B **70**, 064101 (2004).
[49] S. M. Nakhmanson, M. B. Nardelli, and J. Bernholc, Phys. Rev. Lett. **92**, 115504 (2004).
[50] J. Bernholc, S. M. Nakhmanson, and M. B. Nardelli, Comput. Sci. Eng. **6**, 12 (2004).
[51] Quantum Design; 11578 Sorrento Valley Road, San Diego, CA 92121.
[52] J. C. Lashley, M. F. Handley, A. Migliori, J. L. Sarrao, P. G. Pagliuso, T. W. Darling, M. Jaime, J. C. Cooley, W. L. Huits, L. Morales, D. J. Thoma, J. L. Smith, J. B.-Goates, B. F. Woodfield, G. R. Stewart, R. A. Fisher, and N. E. Phillips, Cryogenics **43**, 369 (2003).
[53] J. S. Hwang, K. J. Lin, and C. Tien, Rev. Sci. Instrum. **68**, 94 (1997).
[54] Apiezon high vacuum greases and waxes (http://www.2spi.com/catalog/vac/apiezon.html).
[55] J. Hone, B. Batlogg, Z. Benes, A. T. Johnson, and J. E. Fischer, Science **289**, 1730 (2000).
[56] Q. M. Zhang, V. Bharti, and X. Zhao, Science **280**, 2101 (1998).
[57] B. Chu, X. Zhao, K. Ren, B. Neese, M. Lin, Q. Wang, F. Bauer, and Q. M. Zhang, Science **313**, 334 (2006).
[58] V. V. Tarasov, Zh. Fiz. Khim. **24**, 111 (1950).
[59] S. F. Kwan, F. C. Chen, and C. L. Choy, Polymer **16**, 481 (1975).
[60] H. Ohigashi, K. Omote, and T. Gomyo, Appl. Phys. Lett. **66**, 3281 (1995).
[61] K. Omote, H. Ohigashi, and K. Koga, J. Appl. Phys. **81**, 2760 (1997).
[62] A. D. Athougies, B. T. Peterson, G. L. Salinger and C. Swartz, Cryogenics **12**, 125 (1972).
[63] A. P. Sokolov, R. Calemczuk, B. Salce, A. Kisliuk, D. Quitmann, and E. Duval, Phys. Rev. Lett. **78**, 2405 (1997).
[64] J. D. Boyer, J. C. Lasjaunias, R. A. Fisher, and N. E. Phillips, J. Non-Cryst. Solids **55**, 413 (1983).
[65] C. L. Choy, W. Y. Leung and F. C. Chen, J. Polym. Sci., Polym. Phys. Ed. **17**, 87 (1979).
[66] T. G. Gibbons, Phys. Rev. B **7**, 1410 (1973).
[67] T. G. Gibbons, J. Chem. Phys. **60**, 1094 (1974).
[68] M. Shen, Polym. Eng. Sci. **19**, 995 (1979).
[69] C. N. Borca, J. Choi, S. Adenwalla, S. Ducharme, P. A. Dowben, L. Robertson, V. M. Fridkin, S. P. Palto, and N. Petukhova, Appl. Phys. Lett. **74**, 347 (1999).
[70] L. M. P. Pinheiro, M. R. Chaud, P. A. P. Nascente, and R. Gregorio, Acta Microscopia **12**, 125 (2003).
[71] R. Gregorio, Jr., M. R. Chaud, W. N. Dos Santos, and J. B. Baldo, J. Appl. Polym. Sci. **85**, 1362 (2002).
[72] F. Rodriquez, *Principles of Polymer Systems* (Taylor & Francis, Washington, DC, 1996).
[73] A. Keller, Rep. Prog. Phys. **31**, 623 (1968).
[74] D. E. Discher and A. Eisenberg, Science **297**, 967 (2002).
[75] H. Assender, V. Blizyuk, and K. Porfyrakis, Science **297**, 973 (2002).
[76] B. Naranjo, J. K. Gimzewski and S. Putterman, Nature (London) **434**, 1115 (2005).
[77] Z. Zhao, J. Li, X. Yuan, X. Li, Y. Zhang, and J. Sheng, J. Appl. Polym. Sci. **97**, 466 (2005).
[78] T. Kajiyama, N. Khuwattanasil, and A. Takahara, J. Vac. Sci. Technol. B **16**, 121 (1998).
[79] Structure Probe, Inc. (http://www.2spi.com/catalog/vac/grease/silicon/free/).
[80] S. B. Lang, *Sourcebook of Pyroelectricity* (Gordon and Breach, New York, 1974).
[81] J. F. Nye, *Physical Properties of Crystals* (Clarendon, London, 1995).
[82] M. E. Lines and A. M. Glass, *Principles and Applications of Ferroelectrics and Related Materials* (Clarendon, London, 2001).
[83] H. Dvey-Aharon and P. L. Taylor, Ferroelectrics **33**, 103 (1981).
[84] A. M. Glass and M. E. Lines, Phys. Rev. B **13**, 180 (1976).